Microwave Studies of the Terrestrial Atmosphere*

Alan H. Barrett

Research Laboratory of Electronics
Massachusetts Institute of Technology
Cambridge, Mass.

Abstract

15768

The basic theory of thermal emission from the terrestrial atmosphere, as applicable to radio frequencies, is presented and utilized to compute the effect of resonance lines of neutral atmospheric constituents. It is shown how ground-based observations of the H_2O line at a wavelength of 1.35 cm can be used to obtain the total integrated H_2O abundance along the line of sight and give information on the H_2O abundance in the stratosphere. Likewise, it is shown that satellite microwave observations can give the integrated H_2O abundance over oceans, but is less promising over land. The spectrum of O_2 is discussed in terms of probing the atmosphere by ground-based, balloon, and satellite observations. Estimates are presented for detecting O_3 and OH by microwave techniques.

---

*This work was supported in part by the U.S. Army, the Air Force Office of Scientific Research, and the Office of Naval Research; and in part by the National Aeronautics and Space Administration (Grant NsG-419).

(NASA 3)

I. Introduction

Studies of the radio properties of the terrestrial atmosphere, stimulated by World War II microwave radar development, tropospheric scattering research, and the more recent need for communication with space vehicles, have led to a considerable amount of published data on how the neutral constituents of the atmosphere affect radio propagation. Early work was devoted to the attenuation by H_2O and O_2 of short centimeter wavelength radiation at, or near, ground level.[1,2] Subsequent investigations have largely continued this trend, at least for millimeter wavelengths. With the advent of low-noise receivers and high-gain antennas, interest has focussed on how the thermal emission properties of the atmosphere might affect radio astronomical observations[3] and satellite communication systems operating at centimeter wavelengths.[4] An excellent bibliography of these subjects, including ionospheric research, with over 1000 listings has been compiled by Nupen[5]; current low-frequency radio astronomical studies of the atmosphere, with many references, are thoroughly covered in the volume by Aarons,[6] and a comprehensive bibliography related exclusively to thermal emission from atmospheric gases at microwave frequencies has been prepared by Abbott and Westwater.[7] Microwave investigations of the sort cited above have been largely dictated by the need for information that is relavent to system design and have not been directed toward using radio methods to obtain data on the physical structure of the atmosphere. However, an increasing amount of research is being devoted to the use of passive radio, particularly microwave, techniques as a means of probing various meteorological and physical phenomena of the atmosphere. For example, one can list microwave refractometer measurements of the variations in refractive index,[8] studies of radio emission from thunderstorm cells,[9] fluctuations in thermal

emission from large-scale weather phenomena such as the passage of a cold front,[10] attempts to detect O_3 by virtue of its resonance lines near 8 mm,[11] a means of detecting high-altitude (stratospheric) H_2O bymmicrowave resonance observations,[12] and use of the O_2 resonance lines at 5 mm as an atmospheric probe. probe.[13,14] The first three programs listed above are concerned with broadband aspects of atmospheric radiation, while the latter three specifically involve spectral resonance lines of atmospheric molecules. This paper will be concerned exclusively with the use of these and other lines, as a means of probing the vertical structure of the atmosphere.

In the wavelength range 1 mm-10 cm, microwave propagation in the earth's atmosphere is dominated almost entirely by the attenuating effects of H_2O and O_2. The principal rotational lines of H_2O in this range are at 22,235 Mc and 183,311 Mc corresponding to wavelengths of 1.35 cm and 1.64 mm, respectively, while the O_2 lines cluster closely near 60,000 Mc with the exception of a single line at 118,745 Mc, that is, at wavelengths of 5 mm and 2.54 mm, respectively. Other atmospheric constituents have microwave lines in this range. The effect of these constituents, however, is at least an order of magnitude smaller than that of H_2O and O_2 because of their small abundance. For this reason, these molecules have not received much attention in propagation studies, but their detection would afford a me means of obtaining geophysical information on the particular species. Atmospheric molecules in this category include O_3, N_2O, CO, OH, NO_2, NO, SO_2, and NH_3. A compilation of the resonant frequencies of these molecules, plus molecules of possible interest in the atmospheres of other planets, has been given previously.[15]

In the following sections the basic theory of absorption and thermal emission from the atmosphere at radio frequencies will be briefly presented, and this will then be applied to the discussion of ground-based, balloon-borne, and satellite

experiments involving atmospheric microwave spectral lines.

II. Thermal Emission and Absorption in the Atmosphere

In the consideration of the transfer of radiation within a gas, a fundamental quantity is the absorption coefficient per unit length, $a(\nu)$, defined by the relation

$$dI_\nu = -a(\nu)\, I_\nu dx, \tag{1}$$

where dI_ν is the change of intensity of radiation at frequency ν in traversing a path of length dx through the gas. The minus sign arises, of course, because the intensity is reduced in its passage through the gas. There will also be emission by the gas which can be represented in terms of a volume emissivity η_ν, defined as the power emitted per unit volume and per unit solid angle. From the requirement of conservation of energy, one is led to the equation of radiative transfer[16]

$$\frac{dI_\nu}{dx} = -a(\nu)\, I_\nu + \eta_\nu. \tag{2}$$

For matter in thermodynamic equilibrium, a condition that certainly will apply for our purposes, the volume emissivity and absorption coefficient are related by Kirchhoff's Law,

$$\frac{\eta_\nu}{a(\nu)} = \frac{2h\nu^3}{c^2}\left(e^{h\nu/kT}-1\right)^{-1} \approx \frac{2kT\nu^2}{c^2}, \tag{3}$$

where the last form of the equation follows from expanding the exponent, since $h\nu/kT \ll 1$. This condition also allows one to express the intensity, or flux density per unit solid angle, I_ν in terms of the brightness temperature T_B defined by the relation

$$I_\nu = \frac{2kT_B\nu^2}{c^2}. \tag{4}$$

Combining these equations, we find that the formal solution to the equation of radiative transfer, Eq. (2), is

$$T_B(h) = T_o\, e^{-\tau_\nu(h,\infty)} + \int_h^\infty T(x)\, e^{-\tau_\nu(h,x)}\, d\tau_\nu, \tag{5}$$

where the optical depth $\tau_\nu(h, x)$, or total attenuation between levels h and x, measured along the line of sight, is given by

$$d\tau_\nu = \alpha(\nu)\, dx \qquad \tau_\nu(h, x) = \int_h^x \alpha(\nu)\, dx \tag{6}$$

Equation (5) admits of an obvious interpretation: The first term represents the contribution at altitude h from a source outside the atmosphere of brightness temperature T_o and attenuated by the entire atmosphere along the line of sight, while the second term is the integrated emission from the atmosphere itself between h and the height at which the atmosphere may be considered nonexistent.

It is clear that any evaluation of thermal emission from the atmosphere must include an expression for the absorption coefficient $\alpha(\nu)$. Practically all microwave results, whether laboratory or atmospheric, are interpreted in terms of the Van Vleck-Weisskopf theory of absorption by collision-broadened lines.[17] This theory gives a general result for the absorption coefficient as follows

$$\alpha(\nu) = \frac{4\pi^3 \nu N}{3ckT} \frac{\sum_j \left[|\mu_{ij}|^2\, \nu_{ij}\, f(\nu_{ij}, \nu)\, e^{-E_j/kT} \right]}{\sum_j e^{-E_j/kT}} \tag{7}$$

$$f(\nu_{ij}, \nu) = \frac{\nu}{\pi \nu_{ij}} \left[\frac{\Delta\nu}{(\nu - \nu_{ij})^2 + \Delta\nu^2} + \frac{\Delta\nu}{(\nu + \nu_{ij})^2 + \Delta\nu^2} \right], \tag{8}$$

where N is the number of molecules per unit volume, E_j is the energy of level j, μ_{ij} is the dipole matrix element connecting states i and j, $\Delta\nu$ is the line width parameter, defined as the halfwidth at half maximum, and ν_{ij} is the resonant frequency defined by levels i and j. In laboratory investigations, the halfwidth might be a few Mc, or less, so that the condition $\Delta\nu/\nu \ll 1$ is satisfied and the second term of Eq. (8) can be neglected. However, in the atmosphere, halfwidths of several thousand Mc are possible and the second term can no longer be dropped.

In atmospheric studies, the largest uncertainty in using the above-given theory arises from the linewidth parameter, $\Delta\nu$. This occurs for two reasons, both of which are connected with the fact that laboratory spectroscopy is carried out under vastly different conditions than are applicable to the terrestrial atmosphere. First, laboratory research is usually carried out with pure samples of a gas; therefore the linewidth parameters so determined are the result of collisions of the species with itself, that is, self-broadening, whereas the linewidth applicable in atmospheric studies results from collisions with several different molecular species. A case in point, the broadening of the O_3 lines by O_3-O_3 collisions is known from laboratory spectroscopy, but the effect of O_3-O_2 and O_3-N_2 collisions will determine the O_3 linewidths in the atmosphere, and the effectiveness of these collisions is unknown. If data are available on foreign gas broadening, the linewidth parameter can be computed from the expression.[18]

$$\Delta\nu_i = \sum_j x_j \Delta\nu_{ij}, \tag{9}$$

where x_j is the fractional abundance of molecule j and $\Delta\nu_{ij}$ is the broadening of the resonance line of molecule i which is due entirely to molecule j. Unfortunately,

however, the $\Delta\nu_{ij}$ are usually unknown and one must rely upon estimates based upon dipole moments or the relative broadening of NH_3 resonances which have been studied with foreign gases.[18] A second uncertainty that arises in applying laboratory data to atmospheric lines is the need for linewidth parameters at pressures of one atmosphere, whereas laboratory data are normally acquired at pressures of 10^{-4}-10^{-5} atmospheres. The laboratory results may be applied over a wide range of pressures, but usually not as high as one atmosphere. The theory of line broadening indicates that linewidths should be proportional to pressure only as long as two-body collisions dominate. When three-body collisions become important, the linewidth will no longer be a linear function of the pressure. Clearly, the pressure when such effects set in will depend on the electrical properties of the interacting molecules and the nature of the interaction responsible for the broadening; therefore general statements applicable to atmospheric situations are difficult. Specific results that apply to H_2O and O_2 will be discussed below.

It is clear from Eqs. (5) and (6) that any evaluation of thermal emission from the atmosphere involves an integration throughout the atmosphere. It is necessary, therefore, to specify how the temperature, pressure, and molecular composition vary along the path of integration. The first two are conveniently given by the compilation of a standard model atmosphere,[19] but the latter will depend on the constituent of interest. For example, the variation of the density of H_2O with height will in no way resemble that of O_2 or O_3. Each case must be treated separately, as will be discussed in Section III.

By means of Eqs. (5)-(8), the optical depth τ_ν' and the brightness temperature T_B in the frequency range from 1 Gc to 100 Gc have been computed for the earth's atmosphere from ground level for zenith angles of 0°, 60°, and 85°. The results are shown in Figs. 1 and 2. The equations have been integrated to a height of 60 km

and include the effect of the earth's curvature. The integrated water vapor abundance assumed is 2 gm/cm^2 distributed exponentially with height and having a ground-level H_2O density of 7.9 gm/m^3. The details of the H_2O and O_2 absorption coefficients used in the computations are given in Sections III and IV.

The qualitative relationship between Figs. 1 and 2 can be understood easily. For example, it is seen from Fig. 1 that the optical depth over the range from 57 Gc to 63 Gc, which is due almost entirely to O_2, is over 100 db for a zenith angle of 0°, that is, the atmoshpere is opaque to these frequencies. This means that any emission received at ground level must originate very near the ground and, therefore, the brightness temperature must be very nearly equal to the temperature at ground level. From Fig. 2 it is seen that this is just the case; over the stated range of frequencies all spectral differences are gone and the brightness temperature equals 285°K, the temperature of the lowest kilometer, or so, of the atmosphere. On the other hand, at 22.2 Gc, the H_2O resonant frequency, the optical depth is no more than 0.6 db, corresponding to a power absorption of 13 per cent, and the atmosphere is relatively transparent and gives rise to only 35°K brightness temperature. Furthermore, the atmospheric 'windows' at 8 mm and 3.5 mm are apparent as minimums in the optical depth curve. The increased optical depth and brightness temperature at zenith angles other than 0° result, of course, from the increased path length through the atmosphere. At 85° zenith angle the H_2O resonance is beginning to be obliterated because of the increase in the total attenuation, much like the case for the O_2 lines between 57 Gc and 63 Gc.

The theory of atmospheric attenuation and emission has been reviewed in this section and used to obtain the general characteristics of the microwave properties of the atmosphere as influenced by H_2O and O_2. In the subsequent sections, the

details of several molecular resonances, including H_2O and O_2, will be investigated in terms of ground-based, balloon-borne, and satellite observations for the purposes of providing meteorological and geophysical information.

III. H_2O Experiments

For the H_2O molecule, Eqs. (7) and (8) can be considerably simplified because most of the H_2O lines are in the infrared. For our purposes, we shall restrict attention to the single line at 22.235 Gc; therefore the equations can be expected to contain a single resonant term plus a term representing the effects of the wings of all the higher frequency lines. If $\nu_{ij} \gg \nu$ and $\nu_{ij} \gg \Delta\nu$, then Eq. (8) can be approximated as $2\nu(\Delta\nu)/\nu_{ij}^3$ for the high-frequency lines. Using this result and inserting numerical values of the molecular parameters in Eq. (7), one obtains[2,12]

$$\alpha(\nu) \approx 1.05 \times 10^{-28} \frac{N\nu^2 e^{-644/T}}{T^{5/2}} \left[\frac{\Delta\nu}{(\nu-\nu_o)^2 + \Delta\nu^2} + \frac{\Delta\nu}{(\nu+\nu_o)^2 + \Delta\nu^2} \right]$$

$$+ 1.52 \times 10^{-52} \frac{N\nu^2 \Delta\nu}{T^{3/2}} \qquad (10)$$

as the absorption coefficient in cm^{-1}. In this expression, ν and $\Delta\nu$ are in sec^{-1}, N is the H_2O number density in cm^{-3}, and T is in °K.

Fortunately, the H_2O line has been investigated in the laboratory in air for pressures of one atmosphere so that many of the uncertainties about $\Delta\nu$, referred to in Section II, are removed.[20] As expected, the principal source of broadening is due to H_2O-O_2 and H_2O-N_2 collisions, but a small contribution comes from H_2O-H_2O collisions in spite of the small relative abundance of H_2O. This is a direct result of the H_2O dipole moment and the large effective collision radius that results therefrom. The H_2O collisions are some five times more effective than the O_2 and N_2 collisions, and, for the most accurate work, this effect must be included. Accordingly, the linewidth is given by

$$\Delta\nu = 1.26 \times 10^{8} \frac{P}{T^{0.625}} \{1 + 4.6 \times 10^{-3} \rho\}, \qquad (11)$$

where P is the total pressure in mm Hg, and ρ is the H_2O density in g/m^3. The temperature dependence of $\Delta\nu$ is that given by Benedict and Kaplan.[21] For T = 300°K and P = 760 mm Hg, the linewidth parameter is 2.7 Gc.

Equations (10) and (11) do not accurately describe H_2O absorption in the atmosphere and, therefore, require modification. Note that Eq. (10) contains a nonresonant term varying as ν^2 and proportional to $\Delta\nu$. This term arises from the approximation made for the absorption in the wings of the high-frequency lines. Experiment has shown that the absorption for frequencies higher than the resonant frequency is larger than that expected from the expressions above, and the reason is not well understood.[2,20,21] However, Eq. (11) was derived from measurements of the 22.2 Gc resonance, but its use in the third term of Eq. (10) implies that all high-frequency lines will have the same broadening. This is contrary to theory[22] and undoubtedly will explain some, if not all, of the discrepancy. In any event, atmospheric measurements can only be explained if the coefficient of the third term of Eq. (10) is increased by a factor of 5 to become 7.6×10^{-52}. This value has been used in all computations reported here.

The contribution of H_2O to the results shown in Figs. 1 and 2 have been computed by using Eqs. (10) and (11). As the frequency approaches the H_2O line at 183.3 Gc, these expressions will be a poor approximation because the condition that $\nu_{ij} \gg \nu$, required for the nonresonant term, will not be satisfied. Therefore, near 100 Gc, Figs. 1 and 2 should be considered approximate only.

Observations of the H_2O line in the terrestrial atmosphere can be used to determine the integrated H_2O abundance along the line of sight. As can be

seen from Fig. 2, the brightness temperature in the neighborhood of the resonant frequency consists of two parts: a resonant term resulting from the first two terms of Eq. (10) and a nonresonant term resulting from the wings of the high-frequency H_2O lines, as given by the third term of Eq. (10), and a small contribution from the wings of the O_2 lines at 60 Gc. By making simultaneous observations at several frequencies over the range 15-35 Gc, it will be possible to determine the brightness temperature T_B and to separate the resonant and nonresonant contributions. The resonant part of T_B follows from Eqs. (5), (6), and (10) as

$$[T_B(\nu)]_{res} = \int_0^\infty T(x)\, d\tau_\nu = \beta\nu^2 \int_0^\infty \frac{Ne^{-644/T}}{T^{3/2}} \cdot \left[\frac{\Delta\nu}{(\nu-\nu_o)^2 + \Delta\nu^2} + \frac{\Delta\nu}{(\nu+\nu_o)^2 + \Delta\nu^2}\right] dx, \tag{12}$$

where $e^{-\tau_\nu(0,x)}$ in the integrand of Eq. (5) has been approximated to be unity because the total optical depth $\tau_\nu(0,\infty)$ is small on the H_2O line, T_o has been taken zero, the lower limit has been set equal to zero as is appropriate for ground-based observations, and $\beta = 1.05 \times 10^{-28}$, the coefficient in Eq. (10). Equation (12) is of little value because of the complicated manner in which it depends on temperature and pressure, since $\Delta\nu$ is a function of both. However, by dividing both sides of Eq. (12) by ν^2 and integrating over the observed line profile, one obtains

$$\int_0^\infty \frac{[T_B(\nu)]_{res}}{\nu^2} d\nu = \beta\pi \int_0^\infty \frac{N(h)\, e^{-644/T}}{T^{3/2}} dh = \beta\pi \frac{e^{-644/T_{avg}}}{T_{avg}^{3/2}} \int_0^\infty N(h)\, dh, \tag{13}$$

where the last equation results from taking the temperature-dependent factors out of the integral and replacing them by an average temperature T_{avg}. Since the integral on the left can be evaluated numerically from the observed line profile, the integrated H_2O abundance can be determined. The main sources of error in this technique will result from errors in determining the line profile and in removing the temperature functions from the integral.

It is seen from Eq. (13) that the area under the brightness-temperature profile is a measure of the total number of H_2O molecules in the line of sight, but gives no information on the manner in which these molecules are distributed with height. However, the vertical distribution of H_2O will strongly influence the shape of the temperature profile[12]; therefore, detailed studies of this shape can give information on the distribution. It might appear that a measure of the brightness temperature on the resonant frequency would be a measure of the total water vapor, but Eq. (12) with $\nu = \nu_o$ shows that the result will depend on the vertical distribution of H_2O through its influence on $\Delta\nu$. In fact, large differences can arise in the value of $T_B(\nu_o)$ for the same integrated abundance, these values depending upon the vertical distribution of H_2O.[12]

The fact that the line shape is drastically influenced by the vertical distribution of H_2O has led to the suggestion that ground-based observations can give evidence of H_2O in the stratosphere.[12] To see how this is possible, consider a distribution of H_2O with height as shown in Fig. 3. Such a distribution is typical of many that have been deduced from balloon flights,[23,24] but there is question as to whether the increase in H_2O abundance above 18 km or so is real or is a result of contamination from the balloon. If the distribution of Fig. 3 is used with the theory of Section II to compute the line profile, the curve of Fig. 4 results. This unusual profile is the result of an exponential

H_2O distribution that gives rise to a profile resembling that of Fig. 2, plus a large response very close to the resonant frequency that originates from the anomolous H_2O abundance above 18 km. Since the 'extra' H_2O is all located at high altitudes, the linewidth for this H_2O is small and the entire effect is concentrated near the resonant frequency. In other words, stratospheric H_2O can only affect the profile near ν_o. The fact that the 'spike' is so large in comparison with the rest of the profile, in spite of the fact that only a minute fraction of the total H_2O is involved, is a result of the absorption at resonance being independent of pressure. This can easily be seen from Eq. (10), since $\alpha(\nu_o) \sim N/\Delta\nu$, which is independent of pressure. Preliminary attempts to detect stratospheric H_2O by this method have been conducted at the Research Laboratory of Electronics, M. I. T., without positive results, but an exhaustive observational effort has not yet been made.

The ground-based experiments discussed above have been concerned with detecting the thermal emission from the atmosphere. The same experiments can be envisioned as absorption experiments with the sun used as a source of background radiation. The analysis follows along the same lines, except that T_o of Eq. (5) would be taken to be the radio brightness temperature at the frequency of interest. Solar absorption observations offer the possibility of detecting smaller effects because the brightness temperature exceeds that of the atmosphere by at least a factor of 20, but there are several disadvantages to solar observations: (1) observations must be restricted to daytime hours, (2) only a limited range of zenith angles is available, (3) interpretation of broad resonances such as the entire H_2O line are complicated by the intrinsic solar radio spectrum, (4) time-variant solar radio events, although rare at microwave frequencies, will hamper the observations, (5) tracking capability

must be available for the observing equipment, and (6) the receiver output fluctuations will be greater. Solar absorption observations appear to offer the greatest improvement for narrow lines, such as the detection of high-altitude H_2O or other constituents found at high altitudes.

Atmospheric H_2O can also be studied by radiometric techniques in conjunction with balloon flights. It is possible to obtain the H_2O distribution with height from such flights by using the same method as used above to obtain the integrated abundance. In this case, however, the integrated abundance could be obtained as a function of height as the balloon rises in the atmosphere, and this, in turn, gives the absolute abundance versus altitude.

Since stratospheric H_2O, if it exists, should be detectable from the ground, it should also be detectable at all heights reached by present balloon technology. By using the H_2O distribution of Fig. 3, the 'spike' on the resonant frequency would have the shapes shown in Fig. 5 for different balloon altitudes. Note that the intensity of the 'spike' becomes larger, at first, as one goes up in the atmosphere, and then decays, but only slowly. It becomes larger because there is less H_2O attenuation between the balloon and the stratosphere as the balloon rises, but it finally begins to decay at the maximum height because there is less H_2O having emission in the frequency range. The decay is also slow because the optical depth is independent of pressure, as discussed above.

As a final topic on H_2O studies, we shall consider possible satellite observations of the H_2O line at 22.2 Gc. The theory of Section II is directly applicable to this situation, except, of course, that the integrations must now be taken from the top of the atmosphere downward to the ground, and T_o in Eq. (5) must be taken to be the brightness temperature of the earth's surface. If the satellite is over land, one can expect T_o to be approximately 290°K, since the emissivity

of the earth will be nearly unity. Approximating Eq. (5) by using an average temperature in the second term gives

$$T_B = T_o e^{-\tau_\nu} + T_{avg}(1-e^{-\tau_\nu}) \tag{14}$$

for a frequency in the H_2O line. On the other hand, for a frequency well removed from the line, Eq. (14) reduces to $T_B = T_o$. Therefore, the brightness temperature difference resulting from the H_2O resonance is simply

$$\Delta T_B = (T_{avg}-T_o)\left(1-e^{-\tau_\nu}\right) \approx (T_{avg}-T_o)\tau_\nu. \tag{15}$$

From Figs. 1 and 2, it is possible to estimate τ_ν as 0.14 and T_{avg} as 260°K. Inserting these values gives $\Delta T_B = 4°K$. This is a small value compared with the emission line of Fig. 2 and does not make this form of a satellite experiment very attractive. The small value results, of course, from the approximate equality between T_o and T_{avg} and the small τ_ν, that is, the absorption of the earth's radiation by the H_2O is almost exactly balanced by the emission from the absorbing gas. More detailed computations of this resonance as seen from a satellite give a brightness temperature change over the H_2O line of 2°K.[15] The line will appear as an absorption line, as represented by the fact that $T_o > T_{avg}$ in Eq. (15).

Although the spectral differences in the brightness temperature caused by H_2O when viewed from a satellite over land will not be large, quite a different situation prevails when the satellite is over the oceans. The radiation to space from the H_2O in the atmosphere will be essentially the same for the two cases, over land or over oceans, because the temperature of the atmosphere is the same, but the brightness temperature T_o of the background surface will be

very different. This difference arises not because the temperatures are different but because the emissivities are different. For example, a typical value for the reflection coefficient of water, at normal incidence, might be 0.5; thus the emissivity would be 0.5; however, for land the reflectivity is low and the emissivity is approximately unity. A second effect of a large reflectivity is that the downward radiation from the atmosphere will be reflected from the water, passed through the atmosphere, and radiated to space. Therefore, one can expect three terms in the equation for the brightness temperature: (1) the upward radiation from the atmosphere directly to space, (2) the radiation from the surface, attenuated by the atmosphere, and (3) the downward radiation from the atmosphere, reflected from the water, and attenuated by the atmosphere. If R is the microwave reflectivity and T_W is the temperature of the water, then the solution of the equation of radiative transfer gives

$$T_B(h_s) = (14R)T_W\, e^{-\tau_\nu(0,h_s)} + \int_{h_s}^{0} T(x)\, e^{-\tau_\nu(x,h_s)}\, d\tau_\nu$$

$$+ Re^{-\tau_\nu(0,h_s)} \int_0^{\infty} T(x)\, e^{-\tau_\nu(0,x)}\, d\tau_\nu, \qquad (16)$$

where h_s is the satellite height. If an average temperature T_{avg} is assumed for the atmosphere, as above, Eq. (16) gives

$$T_B(h_s) = (1-R)T_W\, e^{-\tau_\nu} + T_{avg}\left(1-e^{-\tau_\nu}\right) + Re^{-\tau_\nu}\, T_{avg}\left(1-e^{-\tau_\nu}\right). \qquad (17)$$

Off resonance, however, $T_B = (1-R)T_W$, as follows from this equation with $\tau_\nu = 0$. Therefore, the spectral response resulting from the H_2O is given by

$$\Delta T_B = \left[\left(1+Re^{-\tau_\nu}\right)T_{avg} - (1-R)T_W\right]\left(1-e^{-\tau_\nu}\right). \qquad (18)$$

If we take $R \tilde{=} 0.5$, $T_W \tilde{=} 290°K$, and use the values of T_{avg} and τ_ν as in Eq. (15), we get $\Delta T_B \tilde{=} 30°K$, a value some 15 times that obtained over land. Note, also, that the line now appears as an emission line because, of course, of the low effective radiative temperature of the water. Detailed computations, by means of Eq. (16), yield the spectrum shown in Fig. 6.

To obtain these results, normal incidence and no frequency variation for the reflectivity R were assumed. In practice, R may be a function of frequency, and this must be incorporated into the equations; however, R will vary monotonically with frequency and does not represent a real problem. For angles other than normal incidence, the reflectivity R will depend on polarization and the degree of roughness of the ocean surface. The latter circumstance opens up the possibility of determining the sea state from passive microwave satellite measurements and relating these to surface wind velocity.

It is possible to approximate Eq. (16) to first order in τ and relate the area under the brightness temperature profile to the integrated H_2O abundance, as in Eq. (13). Therefore, passive microwave measurements from a satellite are capable of allowing a determination of the total H_2O content of the atmosphere over oceans. The same experiment over land appears to be less promising; however, meteorological data over the oceans are far more lacking than over land. The great value of the microwave method over other techniques, for example, infrared, is that many clouds are relatively transparent to microwave frequencies, or their effect on the resonant part of the brightness temperature $[T_B(\nu)]_{res}$ can be subtracted easily from the observed spectrum. A second advantage is that in the microwave range one deals with a single, optically

thin line, whereas in the infrared range one has many overlapping lines of large optical depth. Therefore, the microwave H_2O line is considerably easier to interpret in terms of integrated H_2O content.

IV. O_2 Experiments

The microwave spectrum of O_2 is considerably more complex than that of H_2O because in the former one must deal with some 30-50 lines of varying intensities, whereas in the latter only 2 lines actually lie in the 10-cm to 1-mm wavelength range. The O_2 molecule is paramagnetic, since it is in a $^3\Sigma$ state, and the interaction of the molecule's permanent magnetic dipole moment with the magnetic field that is set up as a result of its rotational motion gives rise to the microwave spectrum. The physical origin of this spectrum, in terms of molecular parameters, has been discussed.[2,18] The equations analogous to Eqs. (10) and (11) have been given recently in a discussion of the O_2 spectrum in the terrestrial atmosphere and will not be repeated here.[14] These equations follow, of course, from the general expressions, Eqs. (7) and (8), and the theory of Section II is applicable to the O_2 spectrum.

It can be seen from Fig. 1 that the optical depth resulting from the O_2 lines at $\lambda = 5$ mm is many times that resulting from the H_2O line at $\lambda = 13.5$ mm. Even though the O_2 lines arise from a magnetic interaction, and hence are inherently weaker than typical electric dipole lines, the large optical depth is due to the combined effect of many overlapping lines and the great abundance of O_2 in the atmosphere. As Figs. 1 and 2 show, O_2 renders the terrestrial atmosphere opaque to 5-mm radiation and precludes the possibility of probing the atmosphere from ground level. However, by observing at frequencies in the wings of the O_2 complex, for example, from 50-55 Gc or 65-70 Gc, the atmospheric attenuation is less than 3 db and individual lines should be discernible.[14] Furthermore, by using the sun as a background source, the effect of the lines will be enhanced, as discussed in Section III. Preliminary results

of an experiment of this type, by observing the line at 53.070 Gc, have been reported[13] and show promise of giving information on temperature changes in the stratosphere.

A basic uncertainty in the theory of the O_2 spectrum in the earth's atmosphere is the linewidth parameter, $\Delta\nu$. As discussed in Section II, this arises from trying to apply laboratory data to the wide range of pressures found in the atmosphere. Experimentally, it has been found that a value of approximately 0.6 Mc/mm Hg is appropriate for pressures near 760 mm Hg, but values of ~ 1.6 Mc/mm Hg are more appropriate in the pressure range 0.25-20.6 mm Hg.[21,25] These numbers simply reflect the fact that one cannot assume pressure broadening to vary linearly with pressure over a ratio of 1000:1. Another uncertainty related to $\Delta\nu$, which has generally been omitted in the calculations of the O_2 spectrum, is that a single value of $\Delta\nu$ is not appropriate to all lines. Many measurements have shown this to be the case,[25] but there is not complete agreement between the measurements, and the exact nature of the variation is obscure.

Studies of the O_2 lines at high altitudes, by using either balloons or satellites, are particularly appealing because individual lines will be resolved and relatively uncontaminated by neighboring lines. For example, at ground level lines have a halfwidth of some 400-500 Mc, whereas the average separation between lines is of the order of 350 Mc. Furthermore, the high vertical attenuation at ground level completely masks any spectral lines in the center of the O_2 complex. On the other hand, at an altitude of 30 km, typical of present-day balloon flights, the halfwidth of the lines is approximately 30 Mc, and the zenith attenuation, for frequencies between resonant lines, is very low, that is, less than 1 db. A typical line profile to be expected at a height of 30 km is shown in Fig. 7 for a series of different zenith angles. The line shown has a resonant frequency

of 61,150.6 Mc and was computed from Eqs. (5) and (6) with $T_o = 0$ and $h = 30$ km; however, the integration was carried out only to 60 km.

When one considers O_2 line profiles at heights of 50 km, or more, considerable caution must be taken in evaluating the theoretical profiles. The linewidth that is due to pressure broadening at these heights has decreased to the point at which competing mechanisms of broadening may no longer be ignored. Two types of broadening become important: (a) Doppler broadening resulting from the random thermal motion of the molecules, and (b) Zeeman broadening resulting from the splitting of each line into its Zeeman components by the geomagnetic field. Computations of line profiles including both these sources of broadening have not been published, but Doppler broadening is included in Fig. 7.

Balloon observations of one or more O_2 lines would be very useful as a means of confirming the predictions of the theory of O_2 emission, particularly with reference to the uncertainties in the pressure-broadened linewidths and the importance of other broadening mechanisms. Furthermore, such studies would determine how sensitive the line intensities and profiles are to temperature variations in the stratosphere, as the ground-level observations seem to suggest.[13] A preliminary attempt to study a single O_2 line in the upper atmosphere was made by the author and his associates when a multichannel radiometer designed to study the line at 61,150.6 Mc was carried aloft on August 22, 1963. The flight, launched at the Balloon Flight Station of the National Center for Atmospheric Research in Palestine, Texas, was of 8 hours duration, of which approximately 6 hours was at a float altitude of 108,000 feet. Data analysis is not complete as this paper is being written, but the results of this flight and subsequent flights will be reported on.

The O_2 lines appear to be particularly well suited for atmospheric soundings by microwave techniques from an earth-orbiting satellite. This is because the O_2 lines are opaque at their resonant frequencies, even at very high altitudes, so that the brightness temperature at that frequency is characteristic of the atmospheric temperature at that height. As the frequency is varied slightly from resonance, the O_2 is less opaque and the received emission originates from a lower level of different atmospheric temperature. Computations give rise to some striking line profiles because of the temperature inversion in the stratosphere,[14] but caution must be exercised in using these results. Near a resonant frequency, the emission will originate from heights in the range 30-70 km, and this is the region in which the Zeeman effect can be expected to be important. This will not only tend to obliterate effects depending upon small frequency differences, but will make the received signal a function of the antenna polarization. Although the Zeeman splitting of the lines in the geomagnetic field will only be approximately 3 Mc, in some cases features of the order of 1 Mc in total width appear in the spectrum; hence the importance of the Zeeman splitting on the resultant spectrum is obvious.

To probe the atmosphere effectively using the O_2 lines as observed from a satellite, one would like to determine the temperature distribution for heights greater than 30 km, since lower heights can be studied by balloon techniques. As can be deduced from Fig. 7, the O_2 above 30 km attenuates very little unless observations are very near a resonant line, in which case the brightness temperature varies strongly with small changes in frequency. This, in turn, implies that to use the O_2 lines to determine the temperature in the upper atmosphere one must use narrow frequency bandwidths and maintain a high degree of frequency stability in the radiometer. Clearly, the smaller the bandwidth the

greater the height resolution that can be obtained. Bandwidths of the order of 1 Mc should be considered; this fact implies a frequency stability that is 5-10 times smaller. The severe frequency stability required poses a difficult instrumentation problem, and the disadvantage inherent in using a narrow bandwidth is a loss of temperature resolution without a corresponding increase in integration time. Nevertheless, these difficulties are not fundamental, and satellite observations of the O_2 lines offer a powerful means to obtain upper-atmosphere temperatures on a global scale. Certainly, wideband measurements are currently feasible and would provide valuable information for future experiments.

V. Experiments Involving Other Molecules

The microwave spectrum of O_3 is rich in lines extending from approximately 10 Gc to the infrared spectrum,[15,26] and therefore O_3 is a prime target for microwave studies. One unsuccessful attempt has been made to detect the line at 36,023 Mc in the terrestrial atmosphere by measuring the atmospheric attenuation as a function of frequency.[11] It is of interest to make a crude estimate of the optical depth as a means of evaluating the expected signal caused by O_3. The line at 37,832 Mc has a maximum absorption coefficient of 7.4×10^{-5} cm^{-1},[26] and, if it is assumed that the O_3 layer is 10 km thick, then $\tau_{O_3} \approx 74\epsilon$, where ϵ is the fractional abundance of O_3. The total number of O_3 molecules is approximately 10^{19} cm^{-2} at a typical height of 20 km; thus ϵ is of the order of 10^{-5}. Hence, $\tau_{O_3} \approx 10^{-3}$ and the expected emission from the atmosphere would be only a few tenths of 1°K. However, if a solar absorption type experiment were performed, the expected signal would be approximately 5°K. Therefore, such an experiment warrants further investigation.

These computations are crude, particularly because the value for the

absorption coefficient utilizes a linewidth parameter determined from O_3-O_3 collisions, whereas one should include effects of O_3-O_2 and O_3-N_2 collisions. These effects will decrease the linewidth and increase the optical depth and thereby make the experiment more feasible.

The detection of other molecules by radio methods seems far less promising than those already discussed. For example, OH has measured radio transitions caused by electronic fine structure extending from 1670 Mc to 37,000 Mc, and one can consider detecting telluric OH known to exist at an altitude of approximately 70 km. However, computations show that 5×10^{14} OH radicals per cm^2 in the $J = 3/2$, $^2\pi_{3/2}$ state are required to give an emission line of 0.05°K at 1667 Mc. This signal is very weak, even by present-day radio astronomical standards, and its detection would require sophisticated equipment. However, the signal can be increased to 5-10°K by using the sun as a background source and increasing the integration time to offset the greater receiver fluctuations that will result. With this technique, one could possibly detect 10^{13}-10^{14} OH radicals per cm^2.

Note from the frequency dependence of Eqs. (7) and (8) that high-frequency lines give a greater attenuation for the same number of molecules along the line of sight. This effect may be offset, at least partially, by the Boltzmann distribution among states at a given temperature, but it suggests that high-frequency lines are more favorable for marginal detections. However, equipment is less sensitive at high frequencies, particularly at millimeter wavelengths, and this makes the detection of millimeter resonance lines difficult. A particularly interesting experiment would be the detection of NO by virtue of its lines at 150,210 Mc and 150,510 Mc because direct experimental evidence for neutral NO in the upper atmosphere is lacking. However, experiments of this nature

must await the development of sensitive spectral line receivers at millimeter wavelengths.

VI. Acknowledgments

The author is indebted to R. J. Allen and D. H. Staelin for assistance with the theoretical computations included herein. All computations were made at the Computation Center, M. I. T.

References

1. R. H. Dicke, R. Beringer, R. L. Kyhl, and A. B. Vane, Phys. Rev. 70, 340 (1946).

2. J. H. Van Vleck, Phys. Rev. 71, 413 (1947); 71, 425 (1947); Propagation of Short Radio Waves, edited by D. E. Kerr (McGraw-Hill Book Company, Inc., New York, 1951), pp. 646-664.

3. T. Orhaug, Publ. Nat. Radio Astron. Obs. Vol. 1, No. 14, pp. 215-250, October 1962; Proc. IEEE 51, 477 (1963).

4. D. C. Hogg and R. A. Semplak, Bell System Tech. J. 40, 1331 (1961).

5. W. Hupen, Technical Note 171, National Bureau of Standards, Washington, D.C., May 1963.

6. J. Aarons, (ed.) Radio Astronomical and Satellite Studies of the Atmosphere, (North-Holland Publishing Company, Amsterdam, 1963).

7. R. L. Abbott and E. R. Westwater, Report 7222, National Bureau of Standards, Boulder, Colorado, December 1961.

8. J. R. Gerhardt and C. M. Crain, Proc. Fifth Weather Radar Conference, pp; 43-44, 1955.

9. R. Fleischer, M. Oshima, T. P. Roark, R. M. Straka, and M. DeJong, Final Report, Contract AF19(604)-8055, Rensselaer Polytechnic Institute, Troy, N. Y., April 30, 1962.

10. V. R. Venugopal, J. Atmos. Sci., September 1963 (in press).

11. R. B. Mouw and S. Silver, Space Sciences Laboratory Report, Ser. 1, No. 1, University of California, Berkeley, June 30, 1960.

12. A. H. Barrett and V. K. Chung, J. Geophys. Research 67, 4259 (1962).

13. W. Kahan, Nature 195, 30 (1962).

14. M. L. Meeks and A. E. Lilley, J. Geophys. Research 68, 1683 (1963).

15. A. H. Barrett, Mem. Soc. Roy. Sci. Liége, Cinq. Ser. 7, 197 (1962).

16. See, for example, S. Chandrasekhar, Radiative Transfer (Oxford University Press, London, 1950); V. Kourganoff, Basic Methods in Transfer Problems (Oxford University Press, London, 1952).

17. J. H. Van Vleck and V. F. Weisskopf, Revs. Modern Phys. 17, 227 (1945).

18. C. H. Townes and A. L. Schawlow, Microwave Spectroscopy (McGraw-Hill Book Company, Inc., New York, 1955).

19. U.S. Standard Atmosphere, 1962, prepared by National Aeronautics and Space Administration, U.S. Air Force, and U.S. Weather Bureau (Government Printing Office, Washington, D.C., 1962).

20. G. E. Becker, and S. H. Autler, Phys. Rev. 70, 300 (1946).

21. A. W. Straiton and C. W. Tolbert, Proc. IRE 48, 898 (1960); 49, 649 (1961).

22. W. S. Benedict and L. D. Kaplan, J. Chem. Phys. 30, 388 (1959).

23. E. Pybus and P. Yunker, J. Geophys. Research 67, 8 (1962).

24. D. G. Murcray, F. H. Murcray, and W. J. Williams, J. Geophys. Research 67, 759 (1962).

25. L. F. Stafford and C. W. Tolbert, J. Geophys. Research 68, 3431 (1963).

26. E. K. Gora, J. Mol. Spectroscopy 3, 78 (1959).

Figure Captions

Fig. 1. The optical depth of the earth's atmosphere versus frequency for zenith angles of 0°, 60°, and 85°.

Fig. 2. The brightness temperature of the earth's atmosphere versus frequency for zenith angles of 0°, 60°, and 85°.

Fig. 3. An idealized H_2O distribution. The departure from an exponential distribution which occurs near 18 km is in doubt and may result from contamination by the balloon used to make the measurements.

Fig. 4. The H_2O frequency profile computed by using the distribution of Fig. 3. The large 'spike' on the resonant frequency results from the anomalous H_2O in the stratosphere.

Fig. 5. The spectra of the 'spike' shown in Fig. 4 as it would appear at various heights in the atmosphere. The distribution of Fig. 3 is assumed with 44 μ of precipitable H_2O above 30 km.

Fig. 6. The H_2O spectra computed for a satellite at a height of 780 km over the ocean. The reflectivity of water is assumed to be 0.5, and the temperature is 300°K. Normal incidence is assumed.

Fig. 7. Computed spectra of the 61,151 Mc line of O_2 for various zenith angles as seen from a height of 30 km.

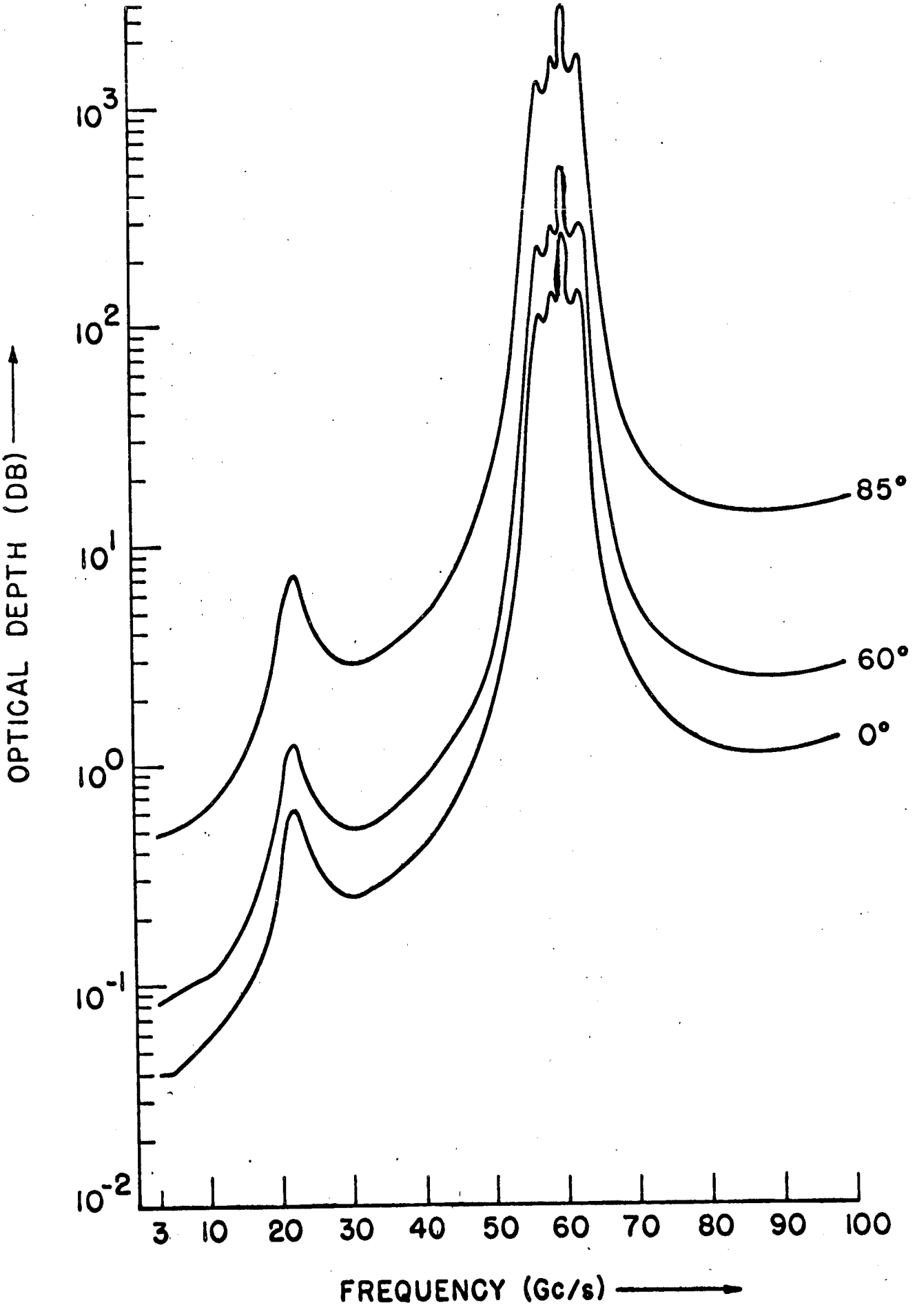
OPTICAL DEPTH (DB)
10^3
10^2
10^1
10^0
10^{-1}
10^{-2}
85°
60°
0°
3
10
20
30
40
50
60
70
80
90
100
FREQUENCY (Gc/s)

Fig. 1

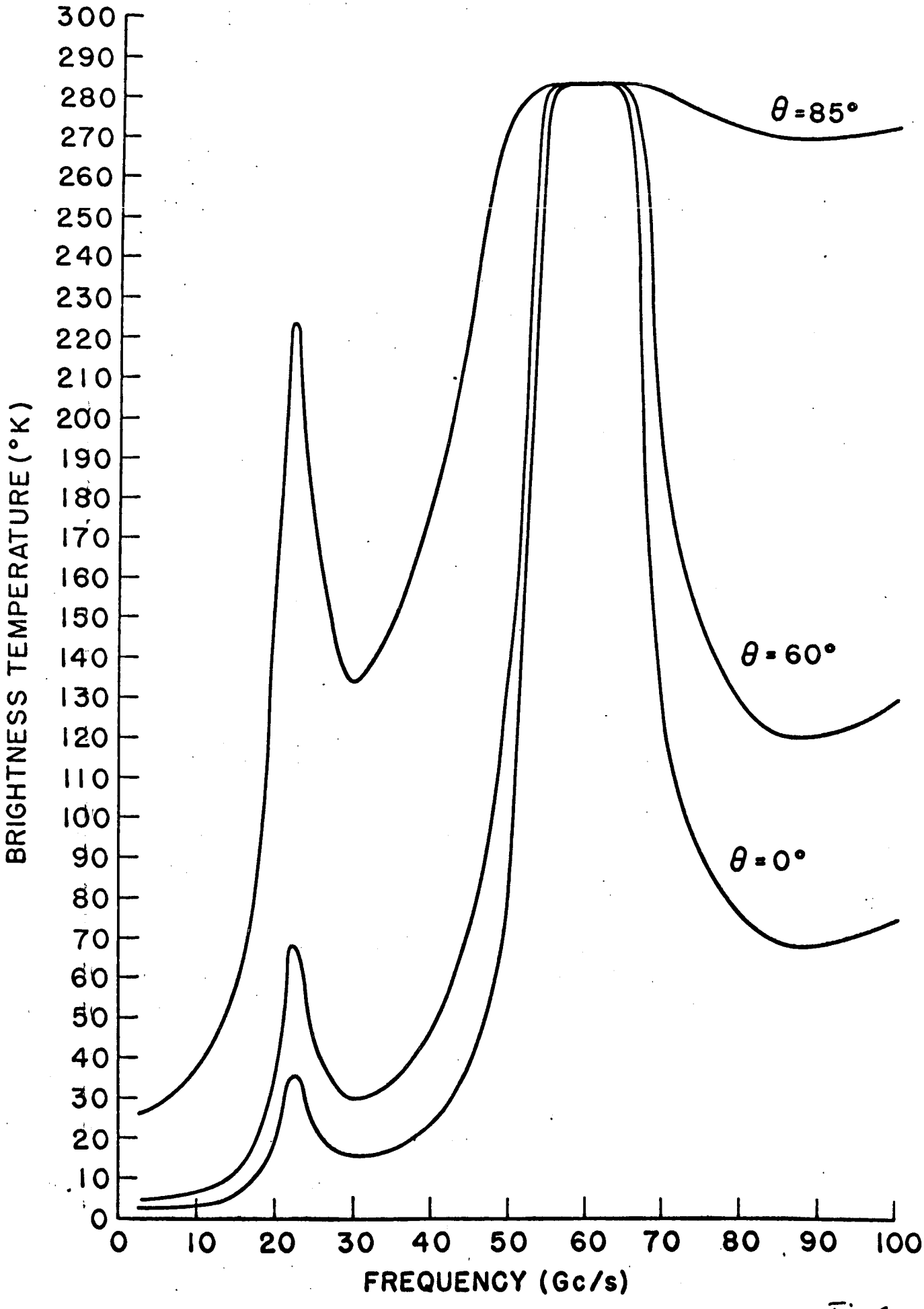
BRIGHTNESS TEMPERATURE (°K)
300
290
280
270
260
250
240
230
220
210
200
190
180
170
160
150
140
130
120
110
100
90
80
70
60
50
40
30
20
10
0
0
10
20
30
40
50
60
70
80
90
100
FREQUENCY (Gc/s)
θ = 85°
θ = 60°
θ = 0°

Fig. 2

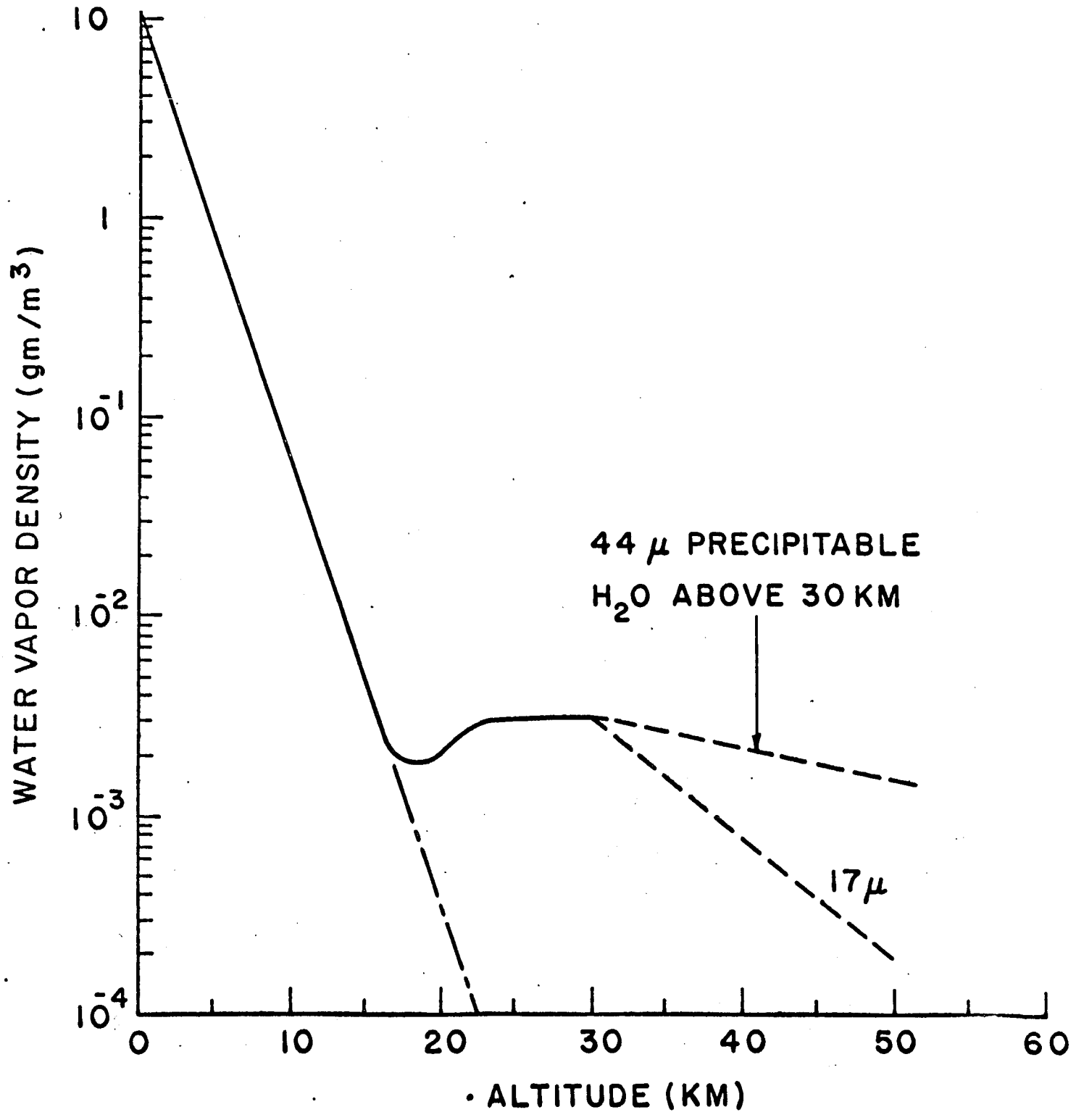
10
1
10^{-1}
10^{-2}
10^{-3}
10^{-4}
WATER VAPOR DENSITY (gm/m^3)
44 μ PRECIPITABLE
H_2O ABOVE 30 KM
17μ
0
10
20
30
40
50
60
ALTITUDE (KM)

Fig. 3

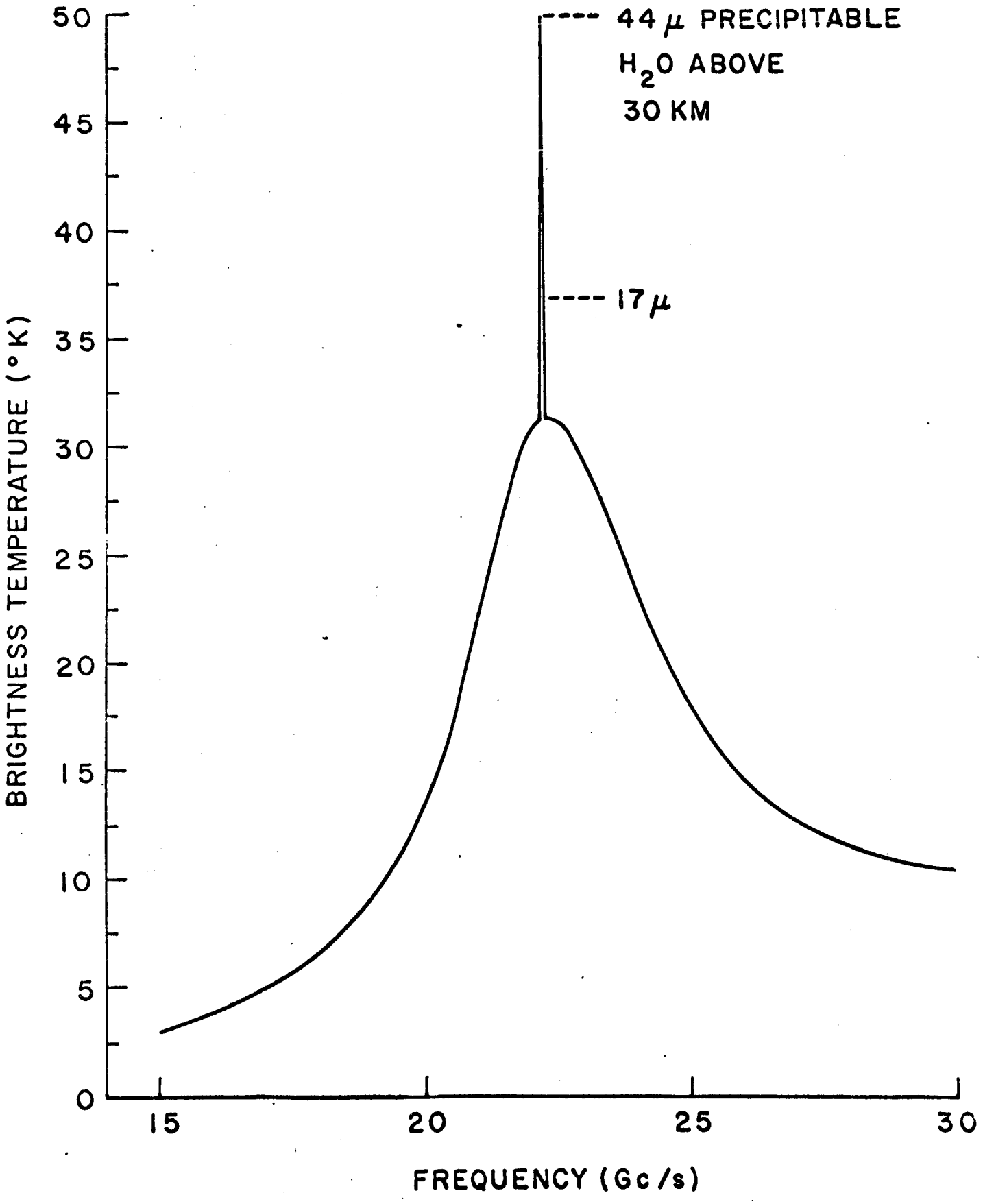
44 μ PRECIPITABLE
H2O ABOVE
30 KM
17 μ
BRIGHTNESS TEMPERATURE (°K)
50
45
40
35
30
25
20
15
10
5
0
15
20
25
30
FREQUENCY (Gc/s)

Fig. 4

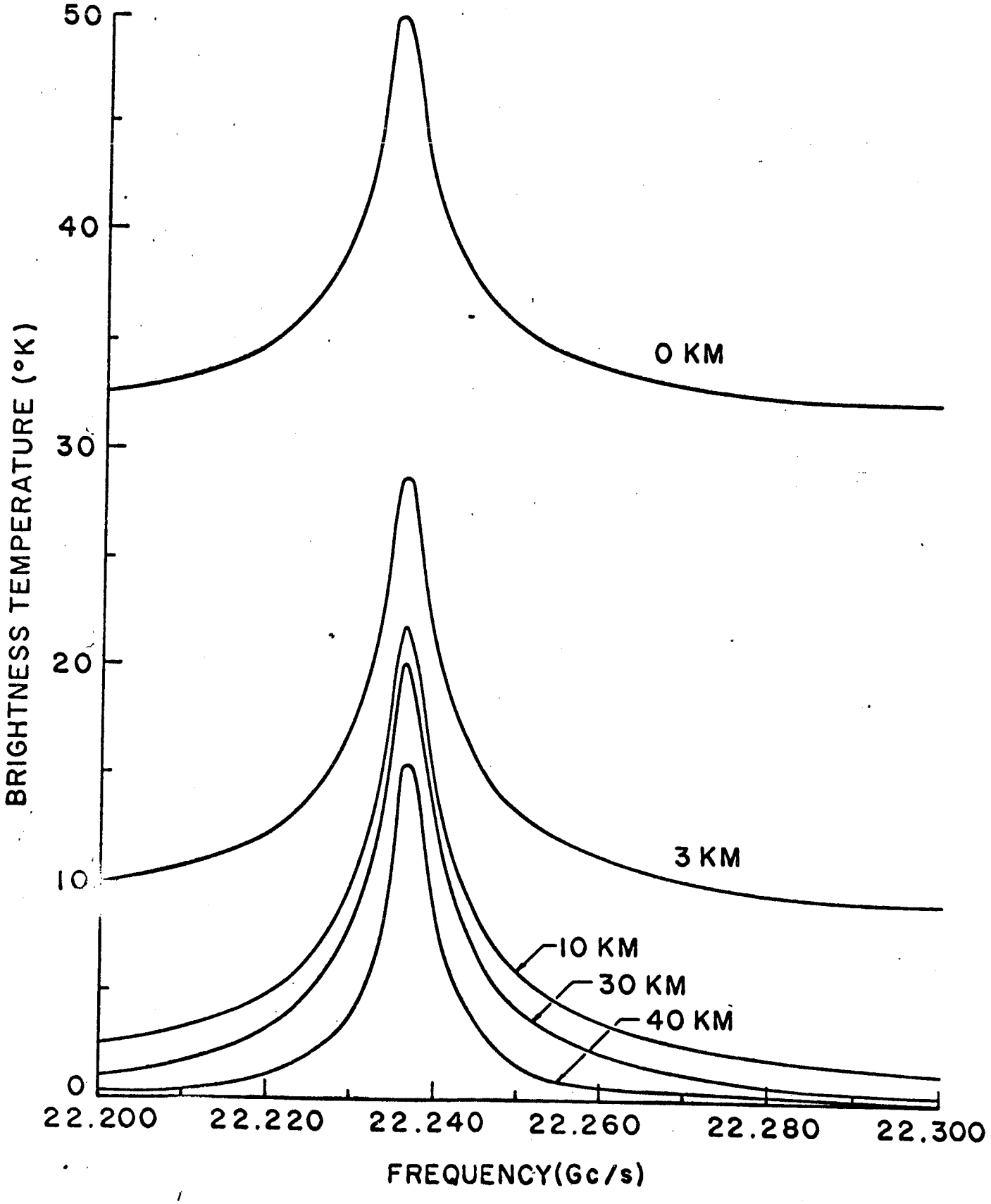
50
40
30
20
10
0
BRIGHTNESS TEMPERATURE (°K)
0 KM
3 KM
10 KM
30 KM
40 KM
22.200
22.220
22.240
22.260
22.280
22.300
FREQUENCY(Gc/s)

Fig. 5

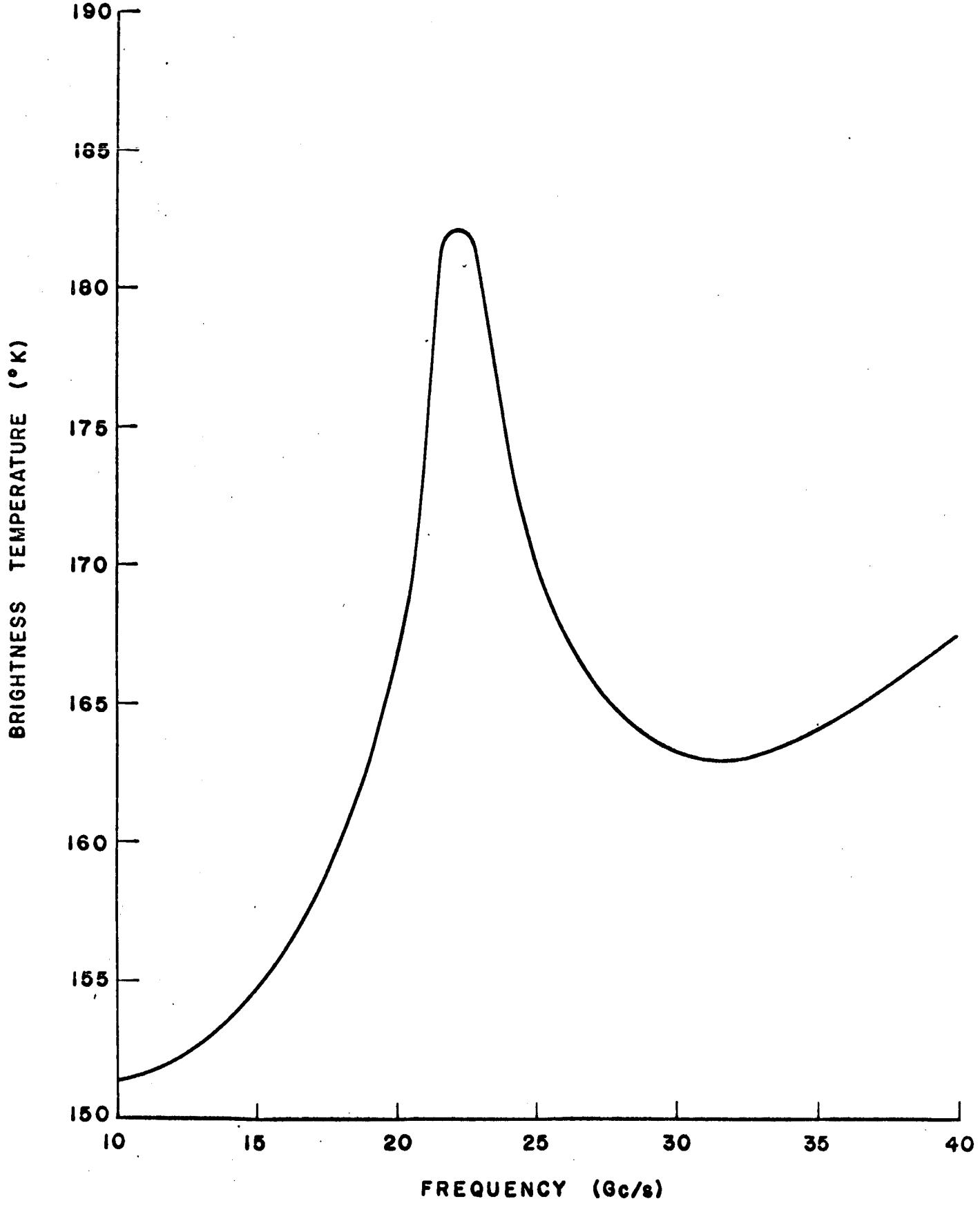
190
185
180
175
170
165
160
155
150
BRIGHTNESS TEMPERATURE (°K)
10
15
20
25
30
35
40
FREQUENCY (Gc/s)

Fig. 6

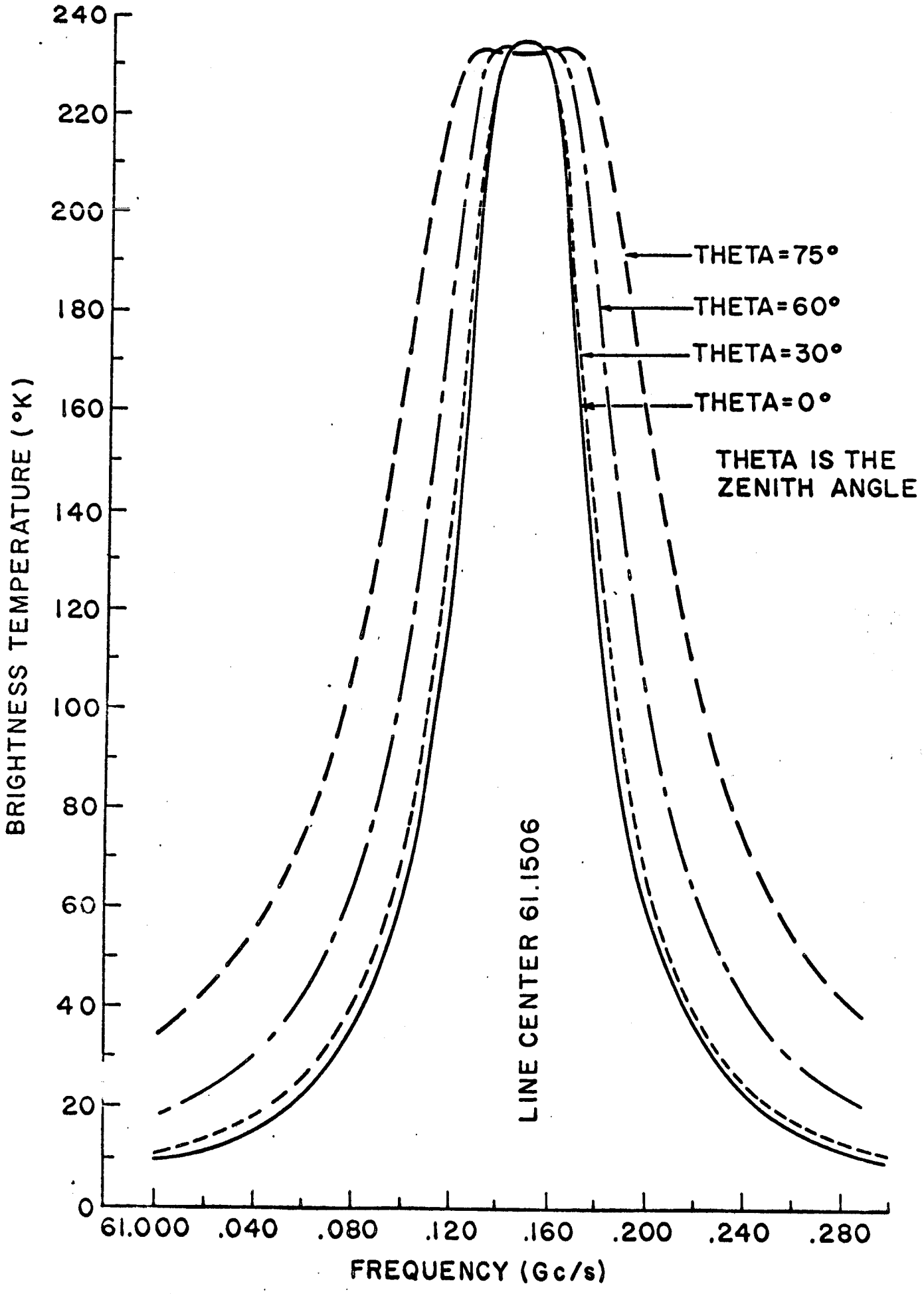
240
220
200
180
160
140
120
100
80
60
40
20
0
BRIGHTNESS TEMPERATURE (°K)
THETA=75°
THETA=60°
THETA=30°
THETA=0°
THETA IS THE ZENITH ANGLE
LINE CENTER 61.1506
61.000
.040
.080
.120
.160
.200
.240
.280
FREQUENCY (Gc/s)

Fig. 7